Scientific Correspondence

Supplementary Text

Low sugar is not always good: Impact of specific *O*-glycan defects on tip growth in *Arabidopsis*

Silvia M. Velasquez[1], Eliana Marzol[1], Cecilia Borassi[1], Laercio Pol-Fachin[2,3], Martiniano M. Ricardi[1], Silvina Mangano[1], Silvina Paola Denita Juarez[1], Juan D. Salgado Salter[1], Javier Gloazzo Dorosz[1], , Susan E. Marcus[4], J. Paul Knox[4], Jose R. Dinneny[5], Norberto D. Iusem[1,6], Hugo Verli[3] & José M. Estevez[1,†]

[1]Instituto de Fisiología, Biología Molecular y Neurociencias (IFIBYNE-CONICET), Facultad de Ciencias Exactas y Naturales, Universidad de Buenos Aires C1428EGA, Argentina.
[2]Departamento de Química Fundamental, Universidade Federal de Pernambuco, Brasil.
[3]Centro de Biotecnologia, Universidade Federal do Rio Grande do Sul, Brasil.
[4]Centre for Plant Sciences, Faculty of Biological Sciences, University of Leeds, Leeds LS2 9JT, UK.
[5]Carnegie Institution for Science, Department of Plant Biology, Stanford, California 94305.
[6]Departamento de Fisiología, Biología Molecular y Celular. Laboratorio de Fisiología y Biología Molecular (LFBM), Facultad de Ciencias Exactas y Naturales, Universidad de Buenos Aires, Buenos Aires C1428EGA, Argentina.

[†] Correspondence should be addressed. Email: jestevez@fbmc.fcen.uba.ar

EXPERIMENTAL PROCEDURES

Plant Materials. *Arabidopsis thaliana* Columbia-0 (Col-0) was used as the wild type (Wt) genotype. Seedlings were germinated on half-strength MS agar plates in a Percival incubator at 22°C in a growth room with 16h light/8h dark cycles for 7-10 days. Plants were transferred to soil for growth under the same conditions as previously described.

T-DNA mutant analysis. For identification of T-DNA knockout lines, genomic DNA was extracted from rosette leaves (Weigel and Glazebrook, 2002). Confirmation by PCR of a single and multiple T-DNA insertions in the target genes SERGT1 (*sergt1-1* SALK_054682 and *sergt1-2* SALK_059879), were performed using an insertion-specific LBb1 (for SALK lines) or Lb3 (for SAIL lines) primer in addition to one gene-specific primer. We isolated homozygous (for all the genes mentioned above). Homozygous *hpat1-1*, *hpat2-1*, and *hpat3-1* (Ogawa-Ohnishi et al., 2013), *xeg113-2* (Gille et al., 2009), *rra3* (GABI_233B05) (Velasquez et al., 2011) and *p4h5* T-DNA mutants (Velasquez et al., 2011) were isolated previously. Double mutants were generated by manual crosses of the corresponding single mutants. The primers used for *sergt1-1* SALK_054682 were: forward 5' GCAGACAAAGAACACTACGGG 3' and reverse 5' CATGAGAGAGAAAGTGGTCCG 3'. For *sergt1-2* SALK_059879, primers were: forward 5' GTGAGCTGTATCTTGGCGAAC 3' and reverse 5' AATCATCCTCCATGCATTGAC 3'. For *p4h5* SALK_152869, primers were: forward 5' CATTTTGAGAGCTCGTTCCAC 3' and reverse 5' TCACAATTTCTTGGTAATTTCGTG 3'. For *rra3* GABI_233B05, primers were: forward 5' GATTCAATATCACAGCCTCGC 3', reverse 5' AACCATGTCATACCTGCAAGC 3'. Primers for *hpat1,2,3* mutants are described elsewhere (Ogawa-Ohnishi et al., 2013).

Root hair phenotypic analysis (shown in **Fig.1 C,E,G**). For quantitative analysis of root hair phenotypes, 200 fully elongated root hairs from the whole root were measured (n roots= 20-30) from seedlings grown on vertical plates on agar 1% with no Murashige and Skoog addition for 7 days under continuous light. Values are reported as the mean ±SD using the Image J software. For measurements of root hair inhibition, P4H inhibitors ethyl-3,4-dihydrohydroxybenzoate (EDHB) (Barnett, 1970) and α,α-dipyridyl (DP)(Majamaa et al., 1986) were added to half-strength MS medium (Velasquez et al., 2011). Fully elongated root hairs (n= 150-200; n roots= 20-30) were analyzed at each P4H inhibitors' concentration. Twenty seedlings of each genotype were measured.

Live imaging of root hair growth and Data Analysis (shown in **Fig. 1I**). Seven-day old seedlings, grown on 0.5% Murashige and Skoog medium 0.7% GelRight under 18hs/6hs light/dark cycles, were imaged for a length of time of 24 hours with images taken every 5 minutes using a macroscopic imaging system described in (Duan et al., 2013). Images were processed by generating a stack of images with ImageJ software (Abramoff et al., 2004), then an algorithm described in (Geng et al., 2013) was used to enhance the contrast of edges, a 200 percent digital zoom was used to amplify selected areas were we could observe root hairs from the

moment of their initiation up to the moment when they stopped growing. The GR was calculated by dividing the total root hair length by the total time of growth. The total time growth was calculated by summing up all of the time points for each root hair (from its initiation to its completion). At least 10 root hairs were analyzed for each mutant.

Root hair EXT immunolabeling. The root surfaces of intact *A. thaliana* seedlings were immunolabeled with monoclonal antibody JIM20 (Smallwood et al., 1994) according to the indirect immunolabeling technique used for intact seedlings. Seedlings were fixed O/N in 4% paraformaldehyde in 50 mM piperazine-N,N-bis(2-ethane-sulphonic acid) (PIPES), 5 mM MgSO4, and 5 mM ethylene glycol tetra-acetic acid (EGTA). Prior to immunolabeling, intact seedlings were incubated in 5% (w/v) milk protein in phosphate-buffered saline (MP/PBS) for 1 h; then incubated in primary antibody JIM20 diluted fivefold in MP⁄PBS for 1.5 h; washed for 3 x for 5 min in PBS; incubated with anti-rat immunoglobulin-G linked to fluorescein isothiocyanate (FITC; Sigma) diluted 100-fold in MP/PBS for 1 h in darkness. After a final washing seedlings were mounted in Citifluor antifade (Agar) and observed on an Olympus BX61 microscope equipped with a Hamamatsu ORCA285 camera and Volocity software (PerkinElmer, Massachusetts, USA).

Co-expression analysis network. Co-expression networks for P4H2, P4H5, RRA3, XEG113 and SERGT1 (cluster 172) were identified from AraNet (http://aranet.mpimp-golm.mpg.de/aranet) and trimmed to facilitate readability. Each co-expression of interest was confirmed independently using the expression angler tool from Botany Array Resource BAR (http://bar.utoronto.ca/ntools/cgi-bin/ntools_expression_angler.cgi) and ATTED-II (http://atted.jp). Only those genes that are connected with genes of interest are included. Co-expression values are based on *Pearson* correlation coefficients where r-value ranges from -1 for absolute negative correlation, 0 for no correlation and 1 for absolute positive correlation.

Molecular Dynamics (MD) simulations of EXT repeat sequence. Carbohydrates and peptides were described under GROMOS96 43A1 force field parameters and GROMACS simulation suite, version 4.0.5 (Hess et al., 2008). The glycan chains and carbohydrate-amino acid connections were constructed based on the most prevalent geometries obtained from solution MD simulations of their respective disaccharides (Pol-Fachin and Verli, 2012). The sequence SPPPPYVYSSPPPPYYSPSPKVYYK was built as a linear peptide, presenting ϕ/ψ backbone torsion angles compatible with type-II polyproline helixes (-75/145 degrees). In order to generate the glycosylated peptides, 4-*trans* hydroxyl groups were added to prolines in SPPPP moieties. Subsequently, *O*-glycosylation sites were filled with their proposed glycan chains, thus generating the initial coordinates for three glycopeptide MD simulations: only arabinosylated EXT, only galactosylated EXT and fully glycosylated EXT (Wt Col-0). In the case of EXT crosslinked sequences, the starting structure for MD simulations was generated by molecular replacement of the non-glycosylated SPPPPYVYSSPPPPYYSPSPKVYYK most prevalent peptide conformation with each chain in collagen three-helix structure in PDB ID 1K6F (Berisio et al., 2002).

Additionally, topologies for the crosslinked Tyr amino acid residues were compiled based on atomic charges, bonded and non-bonded parameters previously present within GROMOS96 43A1 force field. Such structures were then solvated in rectangular boxes using periodic boundary conditions, in which a covalent peptide bond was defined between the Ser and Lys amino acid residues at the box edge on the z-axis of SPPPPYVYSSPPPPYYSPSPKVYYK simulations, thus treating such polypeptide chains as “infinite” polymers. The employed MD protocol was based on a previous study (Velasquez et al., 2011), in which such simulations were extended to 100 ns.

LEGENDS TO FIGURES

Figure S1. A Post-translational modification steps of EXT and EXT-related proteins. Only the repetitive sequence Ser-(Pro)4 is shown. P4Hs converts peptidyl-Pro into Hyp. Hyp is then glycosylated by the sequential addition of arabinosyl units by arabinosyltransferases HPAT1-3, RRA3 and XEG113. In addition, Ser is mono-*O*-galactosylated by SERGT1. **B.** Arabinosylation of small peptides with up to three arabinose units. HPAT3 arabinosylates the small secreted peptide CLAVATA3. It is proposed that RRA3 and XEG113 would add the second and third arabinose unit.

Figure S2. Growth parameters and root hair length of *O*-glycan deficient mutants and 35S-P4H5 OX. **A.** Growth, **B** final growth time and **C** root hair length of Wt, *O*-glycosylation deficient mutant lines (*p4h5*, *sergt1*, *p4h5 sergt1*, *xeg113*) and P4H5 overexpressor line. P values of one-way analysis of variance (ANOVA) test, (*) $P < 0.01$, (***) $P < 0.001$. NS= not significant.

Figure S3. *O*-Glycosylation effect on EXT conformation. **A.** Representative frames from non-hydroxylated (black), *O*-galactosylated (red), *O*-arabinosylated (green) and Wt Col-0 glycosylation state (blue) of EXT minimal peptide in MD simulations, obtained as the most prevalent group from a clustering analysis on the entire trajectory with a 0.8 nm cutoff. In the structures, the peptide is shown as cartoon, Tyr residues are presented as sticks and *O*-linked glycan chains as dots. **B.** Distance between Tyr6:$C_\xi 2$ and Tyr8:OH during molecular dynamics simulations of SPPPP**Y**V**Y**SSPPPPYYSPSPKVYYK peptides.

Table S1. Biological properties of the enzymes involved in the posttranslational modifications of HRGPs.

Gene (AGI)/ CAZy	*Mutant*	*In vitro* activity	Subcellular localization	Tissue localization	Enzyme activity/ mutant phenotype	Reference
Prolyl 4-Hydroxylases (P4Hs)						
P4H2 (AT3G06300)	*p4h2-1; p4h2-2*	Yes	ER, Golgi	Root, Root Hairs	ND/ Short root hairs.	(Velasquez et al., 2011) (Tiainen et al., 2005)
P4H5 (AT2G17720)	*p4h5*	Yes	ER, Golgi	Root, Root Hairs	EXT proline-peptidyl hydroxylation / Short root hairs.	(Velasquez et al., 2011) (Velasquez et al., 2014)
P4H13 (AT2G23096)	*p4h13*	-	ER, Golgi	Root, Root Hairs	ND /Short root hairs.	(Velasquez et al., 2011)
Arabynosyltranferases (AraTs)			-	-		
AtHPAT1 (AT5G25265) GT8 AtHPAT2 (AT2G25260) GT8 AtHPAT3 (AT5G13500) GT8	*hpat1-1* *hpat2-1* *hpat3-1*	Yes Yes Yes	Golgi	Root Hairs	Hyp-O-arabinosyltransferase / impaired pollen tubes growth enhanced hypocotyl elongation, and early flowering. Short root hairs	(Ogawa-Ohnishi et al., 2013) This study
AtRRA1 (At1g75120) GT77 AtRRA2 (At1g75110) GT77	*rra1* *rra2*	ND ND	Golgi	-	ND/ Short root hairs. Reduced levels of arabinose in the mutant	(Petersen et al., 2011) (Egelund et al., 2007)
AtRRA3 (At1g19360) GT77	*rra3*	ND	Golgi	Root Hairs	ND/ Short root hairs. Reduced levels of arabinose in EXTs present in the mutant.	(Velasquez et al., 2011)
AtXEG113 (At2g35610) GT47	*xeg113-2*	ND	Golgi	Root Hairs	ND/ Short root hairs. Reduced levels of arabinose in the mutant	(Gille et al., 2009) (Velasquez et al., 2011)
Galactosyltranferase (GalT)						
AtSERGT1 (At3g01720) GT96	*sergt1-1; sergt1-2*	Yes	Unknown	Root, Root Hairs	Serine galactosyltransferase activity/Short root hairs. Reduced levels of galactose in the mutant	(Saito et al., 2014) This study

ND= not detected.

References

Abramoff MD, Magalhaes PJ, Ram SJ (2004) Image processing with ImageJ. Biophotonics international **11:** 36-43

Barnett NM (1970) Dipyridyl-induced Cell Elongation and Inhibition of Cell Wall Hydroxyproline Biosynthesis. Plant Physiol **45:** 188-191

Berisio R, Vitagliano L, Mazzarella L, Zagari A (2002) Crystal structure of the collagen triple helix model [(Pro-Pro-Gly) 10] 3. Protein Science **11:** 262-270

Duan L, Dietrich D, Ng CH, Chan PMY, Bhalerao R, Bennett MJ, Dinneny JR (2013) Endodermal ABA signaling promotes lateral root quiescence during salt stress in Arabidopsis seedlings. The Plant Cell Online **25:** 324-341

Egelund J, Obel N, Ulvskov P, Geshi N, Pauly M, Bacic A, Petersen B (2007) Molecular characterization of two *Arabidopsis thaliana* glycosyltransferase mutants, *rra1* and *rra2*, which have a reduced residual arabinose content in a polymer tightly associated with the cellulosic wall residue. Plant Mol Biol **64:** 439-451

Geng Y, Wu R, Wee CW, Xie F, Wei X, Chan PMY, Tham C, Duan L, Dinneny JR (2013) A spatio-temporal understanding of growth regulation during the salt stress response in Arabidopsis. The Plant Cell Online **25:** 2132-2154

Gille S, Hansel U, Ziemann M, Pauly M (2009) Identification of plant cell wall mutants by means of a forward chemical genetic approach using hydrolases. Proc Natl Acad Sci U S A **106:** 14699-14704

Hess B, Kutzner C, Van Der Spoel D, Lindahl E (2008) GROMACS 4: Algorithms for highly efficient, load-balanced, and scalable molecular simulation. Journal of chemical theory and computation **4:** 435-447

Majamaa K, Gunzler V, Hanauske-Abel HM, Myllyla R, Kivirikko KI (1986) Partial identity of the 2-oxoglutarate and ascorbate binding sites of prolyl 4-hydroxylase. J Biol Chem **261:** 7819-7823

Ogawa-Ohnishi M, Matsushita W, Matsubayashi Y (2013) Identification of three hydroxyproline O-arabinosyltransferases in Arabidopsis thaliana. Nat Chem Biol **9:** 726-730

Petersen BL, Faber K, Ulvskov P, Ulvskov P (2011) Glycosyltransferases of the GT77 family. Annual Plant Reviews: Plant Polysaccharides, Biosynthesis, and Bioengineering**:** 305-320

Pol-Fachin L, Verli H (2012) Structural glycobiology of the major allergen of Artemisia vulgaris pollen, Art v 1: O-glycosylation influence on the protein dynamics and allergenicity. Glycobiology **22:** 817-825

Saito F, Suyama A, Oka T, T Y-O, Matsuoka K, Jigami Y, Shimma Y (2014) Identification of novel peptidyl serine *O*-galactosyltransferase gene family in plants. J Biol Chem **DOI. 10.1074/jbc.M114.553933**

Smallwood M, Beven A, Donovan N, Neill SJ, Peart J, Roberts K, Knox JP (1994) Localization of cell wall proteins in relation to the developmental anatomy of the carrot root apex. The Plant Journal **5:** 237-246

Tiainen P, Myllyharju J, Koivunen P (2005) Characterization of a second Arabidopsis thaliana prolyl 4-hydroxylase with distinct substrate specificity. J Biol Chem **280:** 1142-1148

Velasquez S, Ricardi M, Dorosz J, Fernandez P, Nadra A, Pol-Fachin L, Egelund J, Gille S, Harholt J, Ciancia M, Verli H, Pauly M, Bacic A, Olsen C, Ulvskov P, Petersen B, Somerville C, Iusem N, Estevez J (2011) *O*-glycosylated cell wall proteins are essential in root hair growth. Science **332:** 1401-1403

Velasquez SM, Ricardi MM, Poulsen CP, Oikawa A, Dilokpimol A, Halim A, Mangano S, Denita Juarez SP, Marzol E, Salgado Salter JD, Dorosz JG, Borassi C, Moller SR, Buono R, Ohsawa Y, Matsuoka K, Otegui MS, Scheller HV, Geshi N, Petersen BL, Iusem ND, Estevez JM (2014) Complex Regulation of Prolyl-4-Hydroxylases Impacts Root Hair Expansion. Mol Plant

Weigel D, Glazebrook J (2002) Arabidopsis: A Laboratory Manual. Cold Spring Harbor Laboratory Press

Figure S1

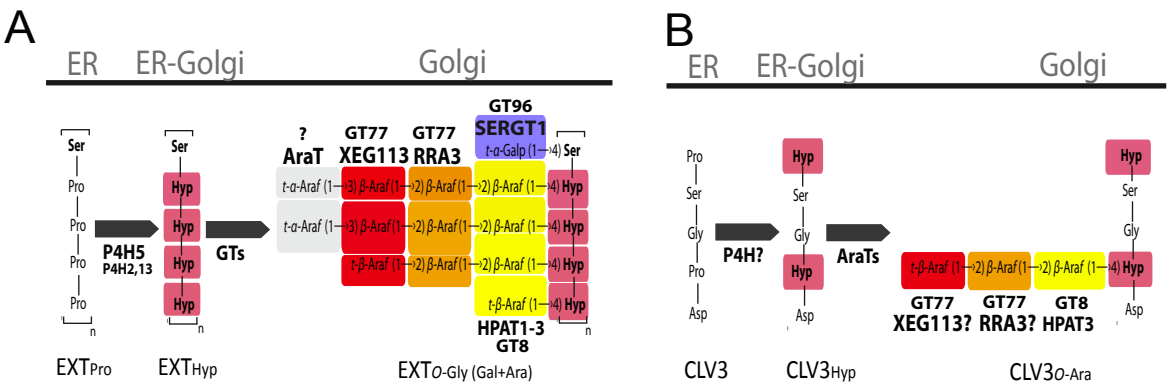

Figure S1. A Post-translational modification steps of EXT and EXT-related proteins. Only the repetitive sequence Ser-(Pro)4 is shown. P4Hs converts peptidyl-Pro into Hyp. Hyp is then glycosylated by the sequential addition of arabinosyl units by arabinosyltransferases HPAT1-3, RRA3 and XEG113. In addition, Ser is mono-*O*-galactosylated by SERGT1. **B.** Arabinosylation of small peptides with up to three arabinose units. HPAT3 arabinosylates the small secreted peptide CLAVATA3. It is proposed that RRA3 and XEG113 would add the second and third arabinose unit.

Figure S2

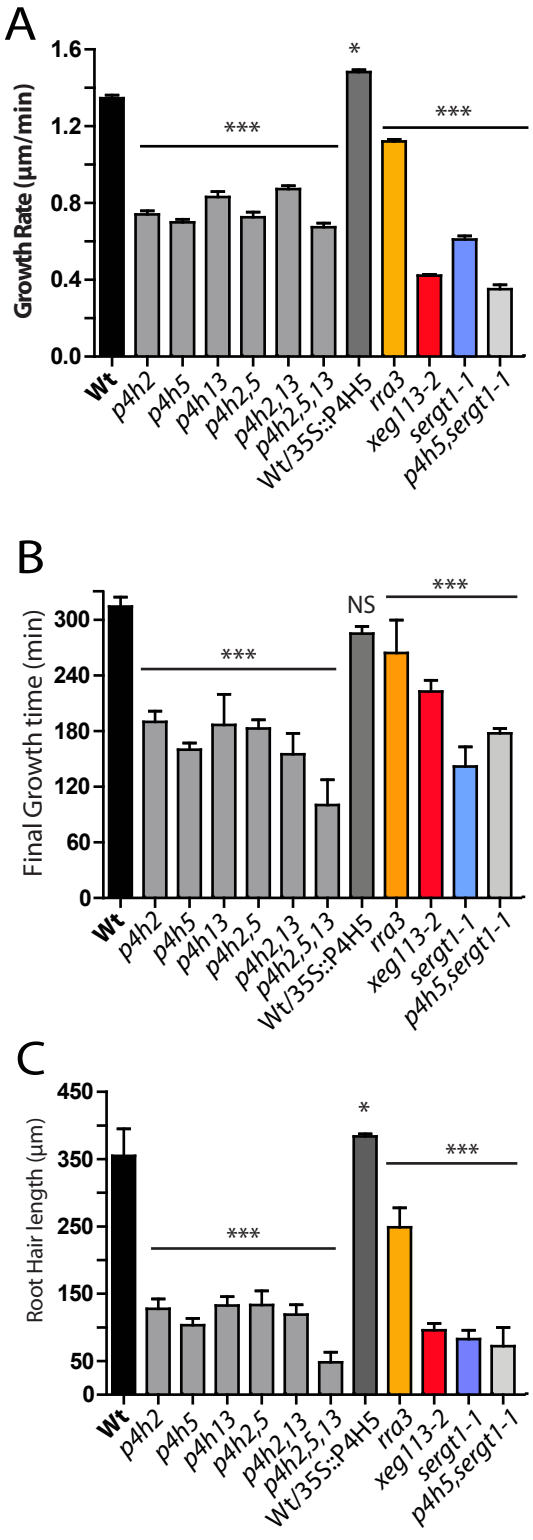

Figure S2. Growth parameters and root hair length of *O*-glycan deficient mutants and 35S-P4H5 OX. **A.** Growth, **B** final growth time and **C** root hair length of Wt, *O*-glycosylation deficient mutant lines (*p4h5*, *sergt1*, *p4h5 sergt1*, *xeg113*) and P4H5 overexpressor line. P values of one-way analysis of variance (ANOVA) test, (*) $P < 0.01$, (***) $P < 0.001$. NS= not significant.

Figure S3

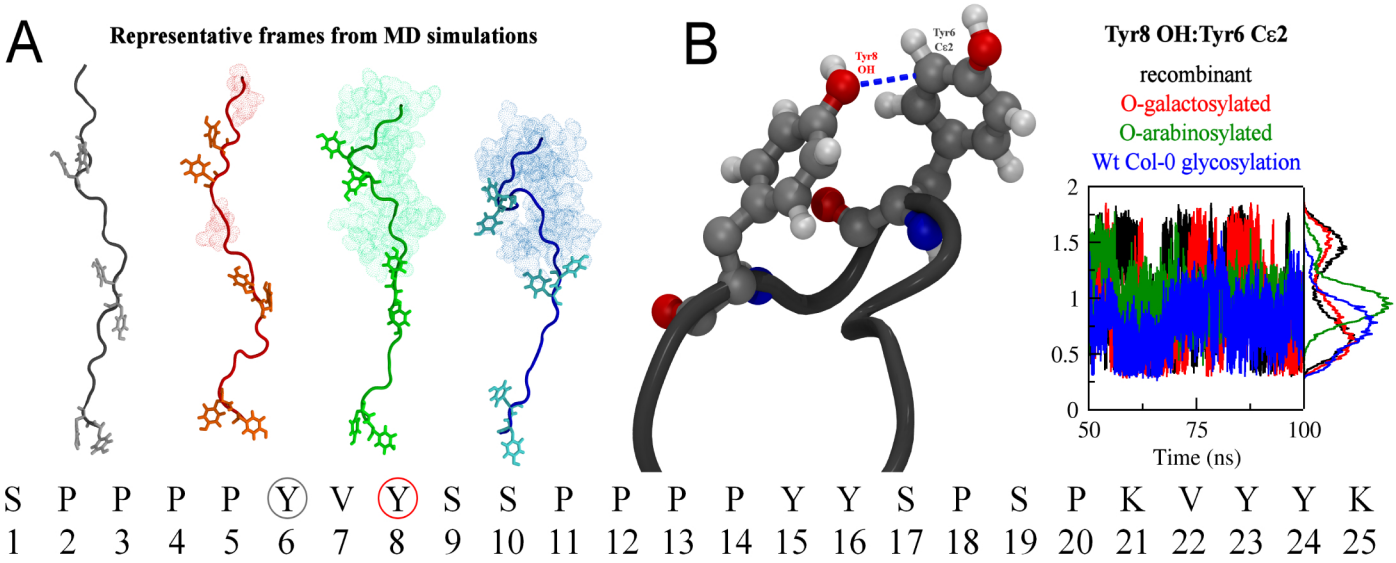

Figure S3. *O*-Glycosylation effect on EXT conformation. **A.** Representative frames from non-hydroxylated (black), *O*-galactosylated (red), *O*-arabinosylated (green) and Wt Col-0 glycosylation state (blue) of EXT minimal peptide in MD simulations, obtained as the most prevalent group from a clustering analysis on the entire trajectory with a 0.8 nm cutoff. In the structures, the peptide is shown as cartoon, Tyr residues are presented as sticks and *O*-linked glycan chains as dots. **B.** Distance between Tyr6:Cξ2 and Tyr8:OH during molecular dynamics simulations of SPPPP**Y**V**Y**SSPPPPYYSPSPKVYYK peptides.